



# Spatial and temporal variability of CO<sub>2</sub>, N<sub>2</sub>O and CH<sub>4</sub> fluxes from an urban park in Denmark

Xiao Bai<sup>1</sup>, Tom Cripps <sup>1</sup>, João Serra <sup>1</sup>, Klaus Butterbach-Bahl <sup>1,2</sup>, and Zhisheng Yao <sup>1,3</sup>

- <sup>1</sup>Pioneer Center Land-CRAFT, Department of Agroecology, Aarhus University, Aarhus, 8000, Denmark
- <sup>2</sup>Institute for Meteorology and Climate Research, Institute for Atmospheric Environmental Research (IMK-IFU), Karlruhe Institute of Technology, Garmisch-Partenkirchen, 82467, Germany
  - <sup>3</sup>State Key Laboratory of Atmospheric Environment and Extreme Meteorology, Institute of Atmospheric Physics, Institute of Atmospheric Physics, Chinese Academy of Sciences, Beijing, 100029, P. R. China
- 10 Correspondence to: Zhisheng Yao (zhishengyao@mail.iap.ac.cn)

**Abstract.** With the rapid worldwide increase in urbanization, urban green spaces are becoming increasingly important in regulating biogeochemical cycles and associated greenhouse gas (GHG) fluxes on regional and global scales. However, the existing data and research on the potential roles of urban green spaces remain limited. In this study, we conducted in situ measurements of nitrous oxide (N<sub>2</sub>O) and methane (CH<sub>4</sub>) fluxes, as well as ecosystem carbon dioxide (CO<sub>2</sub>) respiration, at 56 sites in a temperate urban park with a hilly landscape during the vegetation and frost-free period as well as the freezethaw period. Based on the arithmetic mean of all the measurements, the soil acted as a source of  $N_2O$  (23.8 ± 1.7  $\mu g$  N m<sup>-2</sup>  $h^{-1}$ ) and a weak sink of CH<sub>4</sub> (-0.26 ± 2.14 µg C m<sup>-2</sup>  $h^{-1}$ ). Over the entire observation period, the mean ecosystem CO<sub>2</sub> respiration was calculated to be 228 ± 18.5 mg C m<sup>-2</sup> h<sup>-1</sup>. High spatial and temporal variability was observed for all three GHGs fluxes, with the coefficient of variation ranging from 45.6-259% for N<sub>2</sub>O, 3154-4962% for CH<sub>4</sub> and 40.3-49.3% for CO<sub>2</sub>, respectively. This variability was primarily associated with changes in soil and environmental factors, including vegetation structure, soil hydrothermal conditions, pH, and the availability of soil carbon and nitrogen. Moreover, random forest models combining the in situ measured data and landscape parameters demonstrated a high probability of identifying spatial patterns and hot or cold spots of GHG fluxes across this heterogeneous landscape. However, the models' performance was limited by the lack of high-resolution soil and vegetation data. Overall, our study provides valuable insights into scaling GHG fluxes in urban green spaces more effectively, enabling a more accurate assessment of how urbanization changes landscape fluxes.

## 1 Introduction

Atmospheric carbon dioxide (CO<sub>2</sub>), methane (CH<sub>4</sub>) and nitrous oxide (N<sub>2</sub>O) are the three important greenhouse gases (GHGs), that significantly impact global warming and atmospheric chemistry (Ravishankara et al., 2009; IPCC, 2013; IPCC, 2021). Microbial processes in soil are major natural sources and sinks of these GHGs (Conrad, 1996; Smith et al., 2018). The strength of these biogenic sources and sinks varies greatly over space and time, and they are expected to respond to



50



environmental and land use changes (van Delden et al., 2016; Feng et al., 2022). Due to rapid worldwide urbanization, soils of urban green spaces, such as parks, gardens, street trees, grassy lawns and wooded areas, are becoming increasingly significant as sources or sinks of these GHGs (van Delden et al., 2018; Zhan et al., 2023). However, in order to determine the realistic global warming potential of soils of urban green spaces, the fluxes of all three GHGs must be accurately quantified and scaled up. Moreover, identifying the drivers of variability in the source/sink strength of these GHGs is also critical for predicting how soils of urban green spaces will respond to climate change in the future.

Unlike natural forests, grasslands, and managed agricultural systems, urban ecosystems may exhibit distinct biogeochemical C and N cycles due to the complex interactions between society and the environment (Kaye et al., 2006). These interactions may result in unique characteristics of CO<sub>2</sub>, CH<sub>4</sub> and N<sub>2</sub>O fluxes from urban green spaces. However, most previous studies on soil GHG fluxes have mainly focused on forests, grasslands, and agricultural ecosystems (Gao et al., 2022; Wangari et al., 2022; Liu et al., 2025; Walkiewicz et al., 2025). Existing studies on GHG fluxes in urban ecosystems have primarily examined CO<sub>2</sub> exchange; while urban soil N<sub>2</sub>O and CH<sub>4</sub> fluxes remain poorly characterized (Jeong et al., 2024; Karvinen et al., 2024; Pan et al., 2024). Braun and Bremer (2018) found that annual N<sub>2</sub>O emissions from various fertilized urban green spaces were between 1.0 and 7.6 kg N ha<sup>-1</sup> yr<sup>-1</sup>, comparable to emissions from intensive agriculture. Despite covering only 6.4% of the investigated land area, Kaye et al. (2004) suggested that urban lawns contribute up to 30% to regional N<sub>2</sub>O budgets. A literature review by Zhan et al. (2023) revealed that soils of urban green spaces generally act as a sink for atmospheric CH<sub>4</sub>, with an average annual uptake of 2.0 kg C ha<sup>-1</sup> yr<sup>-1</sup>. However, this magnitude is relatively low compared to the annual CH<sub>4</sub> uptake by other non-urban soils and would decrease further with increased urbanization (Zhang et al., 2021).

Urbanization involves a transition from natural and managed ecosystems to urban green spaces, which alters environmental and soil conditions, such as soil texture, pH, nutrient availability and hydrothermal dynamics (Kaye et al., 2006; Edmondson et al., 2016; Zhan et al., 2023). These factors, acting alone or in combination, lead to high spatial and temporal variability in soil GHG fluxes. This variability limits the ability of researchers to constrain regional and global emission inventories. Currently, the uncertainty associated with most estimates of GHG fluxes from urban soils is often substantial, as the spatial and temporal variations of urban soil fluxes are not well understood. Furthermore, such high uncertainty hinders the identification of the primary drivers of spatiotemporal variability.

Denmark, which consistently ranks among the top three happiest nations in international well-being surveys. It has a higher per capita provision of urban green spaces (61.7 m² per capita) than the global average (Statistics Denmark, 2021). This provides a valuable opportunity to examine the biogeochemical significance of urban green spaces for humans and the environment. Numerous studies have emphasized the various ecosystem services provided by urban green spaces, such as environmental services (e.g., mitigating elevated urban heat and pollution), ecological services (e.g., sustaining urban wildlife habitats and biodiversity conservation), and social and human health benefits (Cardinali et al., 2024; Poulsen et al., 2024). However, no studies have yet reported measurements of in situ soil GHG flux from urban green spaces in Denmark. Therefore, the aim of this study was to quantify and characterize the spatial and temporal variability of soil N<sub>2</sub>O, CH<sub>4</sub> and

https://doi.org/10.5194/egusphere-2025-5091 Preprint. Discussion started: 18 November 2025

© Author(s) 2025. CC BY 4.0 License.





 $CO_2$  fluxes, using a large number of sampling sites (n = 56) spread across an urban park in Aarhus, Denmark. Furthermore, we assessed the role of environmental and soil variables (e.g., topography, soil temperature, moisture, pH, soil organic C, total N and pH) as the main drivers of these spatiotemporal patterns. We also used a machine learning-based upscaling framework to predict the potential GHG hot spots and cold spots.

#### 2 Materials and methods

## 2.1 Study area

70

80

The study area is located within Aarhus University Park (AU Park) in the center of Aarhus, Denmark (56.168°N, 10.203°E) (Fig. 1). The region has a temperate oceanic climate (Cfb, Köppen classification), which is characterized by warm and humid summers and cold and damp winters. The area's long-term average annual precipitation is 1046.3 mm, and its mean annual temperature is 8.8 °C (Danish Meteorological Institute, http://www.dmi.dk). Mean daily temperatures range from a minimum of -14.6 °C to a maximum of 26.4 °C, with frequent frost occurring in the winter months. AU park is situated in a hilly landscape that is part of an old moraine valley extending from Katrinebjerg in Vejlby in the north to the Bay of Aarhus in the east. The park area is dominated by grass-clover lawns that are occasionally mowed and interspersed with old oak trees (*Quercus robur*) that are over 80 years old. Two artificial ponds have been created in the lower part of the park and are fed by a small stream that comes from a spring inside the park.

To better understand the spatial and temporal variability of CO<sub>2</sub>, CH<sub>4</sub> and N<sub>2</sub>O fluxes, 56 sampling sites were selected across the AU park. These sites were chosen for their varied landscape configurations and pond areas, representing different microtopographic and soil moisture conditions.

The soils in the study area are typically luvisols (Adikhari et al., 2014), with a sandy loam to loamy texture in the topsoil that developed on moraine sand (Pedersen et al., 1989). However, since AU park is surrounded by university buildings established in the 1930s and a full soil survey was beyond the scope of this study, we assume that the park's soils have been affected by the incorporation of building materials and landscaping. This has resulted in altered soil profiles and soil properties compared to "natural" soils (Vasenev and Kuzyakov, 2018). No fertilizer was applied during the measurement periods.







Figure 1: The map showing the land cover types and the locations of the sampling sites across a city park at Aarhus University.

# 2.2 Measurements of CO<sub>2</sub>, CH<sub>4</sub> and N<sub>2</sub>O fluxes

90

Fluxes of  $CO_2$ ,  $CH_4$  and  $N_2O$  were measured using the fast-closed chamber technique, as described by Hensen et al. (2013) and Daelman et al. (2025). The opaque chamber was 20 cm high and 37.5 cm in diameter. It contained a small fan inside to



100

110

115

120

125



mix the air in the chamber and a 1 m long, 1/8" wide ventilation tube at the top of the chamber for pressure equalization. Instead of using pre-installed ground frames, we carefully pushed the chamber, with its sharpened and polished bottom edge, about 1-2 cm directly into the ground for flux measurements. To ensure that each flux measurement was always taken from the same plot at the sampling site, we inserted a small metal plate (approximately 1 x 1 cm) into the soil and used a metal detector to locate the plate and identify the site.

During the vegetation and frost-free period (20 July to 9 November, 2023) and the freeze-thaw period (22 November to 7 December, 2023), flux measurements were performed weekly at all 56 sampling sites, using two portable infrared gas analyzers: one measuring N<sub>2</sub>O concentrations (LI-7820, LI-COR Biosciences, Lincoln, NE, USA) and the other measuring CH<sub>4</sub> and CO<sub>2</sub> concentrations (LI-7810, LI-COR Biosciences, Lincoln, NE, USA) (Fig. S1). On each sampling day (8:00-16:00), we used a chamber closure time of 5-7 min, and we monitored the change in headspace GHG concentrations by circulating headspace air between the chamber and the analyzers at a rate of approximately 200 ml min<sup>-1</sup>. Fluxes with units mass N m<sup>-2</sup> h<sup>-1</sup> for N<sub>2</sub>O and mass C m<sup>-2</sup> h<sup>-1</sup> for CH<sub>4</sub> and CO<sub>2</sub> were then calculated based on the decrease or increase of headspace GHG concentrations over time using Eq. (1), which combines the ideal gas law and scaling variables:

$$F = \frac{dq}{dt} * \frac{P*V*M}{R*T*A} (1)$$

Where dq/dt represents the rate of change of gas mixing ratios with time (h<sup>-1</sup>), *P* is the atmospheric pressure (atm), V is the chamber volume (m<sup>3</sup>), M is the molar mass of the gas (mass mol<sup>-1</sup>), R is the universal gas constant (m<sup>3</sup> atm K<sup>-1</sup> mol<sup>-1</sup>), T is the air temperature (K), and A is the chamber area (m<sup>2</sup>). Note that the CO<sub>2</sub> emissions represent ecosystem respiration (ER-CO<sub>2</sub>) because all above-ground biomass were trapped in the opaque chambers during the measurements, so the measured changes in chamber headspace CO<sub>2</sub> concentration were due to both soil and plant respiration.

Soil temperature and volumetric water content at a depth of 5 cm were measured in the direct vicinity of each sampling chamber site alongside each flux measurement using a combined temperature and moisture sensor. Data collection and storage were controlled by HOBO Data Logging Solutions (Onset, 1-800-LOGGERS).

#### 2.3 Soil sampling and properties

At the end of the experimental period, topsoil samples (0-10 cm) were collected from the center of each sampling site using a soil auger. Part of the soil samples were used to measure soil ammonium (NH<sub>4</sub><sup>+</sup>) and nitrate (NO<sub>3</sub><sup>-</sup>) concentrations. After extraction of fresh soil samples with 1M potassium chloride (KCl) solution in a soil:solution ratio of 1:2, soil NH<sub>4</sub><sup>+</sup> and NO<sub>3</sub><sup>-</sup> concentrations were analyzed using an AA500 AutoAnalyzer (Seal Analytical) (Best, 1976, Crooke and Simpson, 1971). Part of the soil samples were dried (60°C, 48h) and sieved (<2 mm) for later analyses of soil total nitrogen (TN), soil organic carbon (SOC) and soil texture.TN was analyzed by dry combustion using a Vario MAX cube (Elementar Analysensysteme AG, Langenselbold, Germany) (Nyang'au et al., 2023). Soil pH was measured in a soil solution with deionized water (soil:solution=1:2) using a pH meter (3110 SET SM Pro, Xylem Analytics Germany GmbH) (Schofield and Taylor, 1955). The clay fraction (<2 μm) and silt fraction (2–20 μm) were quantified using the hydrometer method. Sand particles larger



130

145

150

155



than 63 µm were separated through wet sieving and SOC was measured using high temperature dry combustion (Schjønning et al., 2023). Besides, soil bulk density (BD) was measured using soil cores and weight measurements of oven-dried soil (105°C, 24h) (Alletto and Coquet, 2009).

#### 2.4 Identification of hot and cold spots of GHG fluxes

In this study, the observed GHG fluxes were classified into three categories: hot spot, cold spot and normal spot. The hot and cold spot thresholds were determined using a formula proposed by Wangari et al. (2023). This formula provides a context-sensitive approach to categorising GHG fluxes by adapting to local conditions rather than relying on fixed absolute thresholds. The classification method was based on the median and interquartile range of the data by Eq. (2) and Eq. (3):

135 Hot spot threshold = M + (Q3 - Q1)(2)

Cold spot threshold = M + (Q3 - Q1)(3)

where M is the median and Q3 – Q1 is the interquartile range of the measured fluxes. Due to the skewed distributions of ER-CO<sub>2</sub> and N<sub>2</sub>O fluxes, the thresholds were such that there were no cold spots. Since CH<sub>4</sub> fluxes can be positive or negative (emissions or uptake), hot spots were areas of high emissions, and cold spots were areas of high uptake.

140 Neither hot spots nor cold spots were classified as normal spots.

#### 2.5 Hot and cold spot upscaling

The hot and cold spots of GHG fluxes observed in the AU park were upscaled using a random forest (RF) model through a two-step approach (Fig. S2).

First, the observational dataset was balanced because the distribution of hot, cold, and normal spots varied substantially across the three gases, with the normal spots category being predominant. This class imbalance could potentially introduce bias, causing the RF model favoring the majority class and fail to accurately identify the minority classes. To address this issue, the minority categories were oversampled during training to improve class balance and reduce prediction bias. We used an ad hoc, iterative approach to identify the most effective oversampling strategy for each GHG (Tables S1-S3).

Second, we used RF for classification with potential predictors of GHG fluxes, including soil physio-chemical properties, vegetation and topography (Table S4). The dataset was randomly divided into a training and internal cross-validation (80%) and external test (20%) sets using a stratified random sampling method. The models were trained and internally validated via 10-fold cross-validation (k=10) performed on the training dataset. We hyper-tuned the models for each GHG using a grid search (Tables S5) according to the log loss. Log loss was selected as a measure of how well the predicted probabilities match the actual class labels, considering both prediction accuracy and confidence.

After hyper-tuning the model, the best performing model was used to rank the different predictors according to their importance (Tables S6-S8). This model was then used for feature selection, during which the least essential variables were removed stepwise according to their rank importance.

https://doi.org/10.5194/egusphere-2025-5091 Preprint. Discussion started: 18 November 2025





160

170

175

180

185



Lastly, the hot and cold spots were spatially upscaled for each GHG, using the final hyper-tuned model (after feature selection) at a monthly time step with a spatial resolution of 0.4 m. To do so, we aggregated the average monthly observations, while also interpolating soil physio-chemical and vegetation predictors using either ordinary kriging or inverse distance weighting for dynamic and temporally static predictors (Table S4). We aggregated all gridded predictors and used the hyper-tuned model to predict the total average classification probability. This created an average probability map showing the likelihood that a location would be classified as a hot spot or cold spot.

## 165 **2.6 Statistical analysis**

The daily fluxes of CH<sub>4</sub>, N<sub>2</sub>O and ER-CO<sub>2</sub> (ER: Ecosystem Respiration) for each sampling date were calculated as the mean of all observed fluxes from the 56 sampling sites. The total cumulative fluxes of CH<sub>4</sub>, N<sub>2</sub>O and ER-CO<sub>2</sub> for each sampling site over a given period (e.g., vegetation and frost-free period) were determined using linear interpolation between measurement dates. To assess the key environmental and soil factors that control the spatial and temporal variation of GHG fluxes, we identified significant (p-value < 0.05) relationships between the GHG fluxes and different variables, specifically site properties, such as soil temperature and moisture, pH, bulk density (BD), soil texture, total nitrogen (TN), and soil organic carbon (SOC). We tested linear, non-linear and multiple regression models based on the stepwise selection of the drivers. For soil pH, we used binned/grouped linear regression. This approach involves dividing the independent variable into discrete bins, calculating the mean of both the independent and dependent variables within each bin and then performing a linear regression on the averaged data (McArdle, 1988). All statistical analyses were performed using R software (version 4.3.2).

#### 3. Results

#### 3.1 Environmental conditions

The length of the observation period was 141 days. Out of those days, 89 had precipitation > 0.2 mm day<sup>-1</sup>, totaling 33.3 mm. Four snow events occurred in late November, resulting in 5-10 cm snow cover, which melted in early December. Over the entire observation period, the mean soil moisture (measured as volumetric water content [VWC]) varied between 21% and 40% (Fig. 2a); while across the 56 sampling sites, the mean VWC ranged from 20% to 51%. The mean air temperature ranged from -9.3°C to 20.4°C, with temperatures <5 °C starting in November. Soil temperature showed a comparable seasonality to air temperature, with values ranging from -0.15°C to 25.5°C (Fig. 2b). Soil properties across the 56 sampling sites exhibited spatial differences (Table S9). For example, SOC ranged from 17-93 g C kg<sup>-1</sup> soil dry weight [SDW], TN ranged from 1-6 g N kg<sup>-1</sup> SDW, the C:N ratio ranged from 10-19, BD ranged from 0.6-1.5 g cm<sup>-3</sup> and pH ranged from 5-8.



190

195

200



# 3.2 Temporal variability of N2O, CH4, and CO2 fluxes

Figures 2c, d, and e illustrate the daily fluxes of N<sub>2</sub>O, CH<sub>4</sub>, and ER-CO<sub>2</sub> from the 56 sampling sites over the vegetation and frost-free periods, as well as the freeze-thaw period.

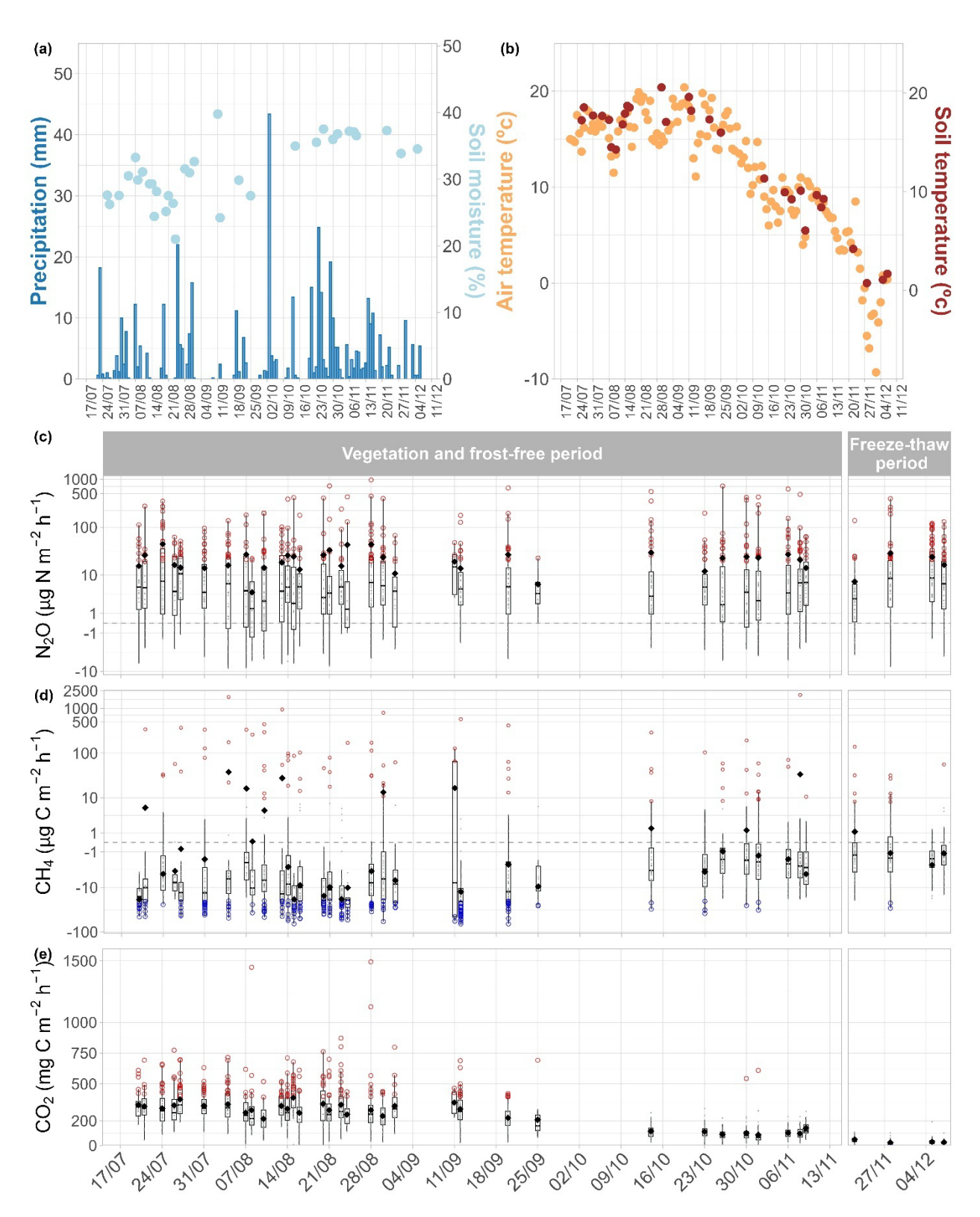
 $N_2O$  fluxes during the entire observation period ranged from 6.3 to 47.0  $\mu$ g N m<sup>-2</sup> h<sup>-1</sup>, with a mean, calculated with all the measurements, of 23.8  $\pm$  1.7  $\mu$ g N m<sup>-2</sup> h<sup>-1</sup>, and a median of 23.6  $\mu$ g N m<sup>-2</sup> h<sup>-1</sup> (Fig. 2c). Higher  $N_2O$  emissions, or  $N_2O$  hot spots ( $\geq$  19.3  $\mu$ g N m<sup>-2</sup> h<sup>-1</sup>), were recorded during both the vegetation and frost-free periods and the freeze-thaw period. The temporal coefficient of variation (CV) for  $N_2O$  fluxes was 45.6% during the measurement period.

CH<sub>4</sub> fluxes ranged from -18.7 to +37.8  $\mu$ g C m<sup>-2</sup> h<sup>-1</sup> during the entire observation period, with a mean, of -0.26  $\pm$  2.14  $\mu$ g C m<sup>-2</sup> h<sup>-1</sup>, and a median of -1.95  $\mu$ g C m<sup>-2</sup> h<sup>-1</sup> (Fig. 2d). Higher CH<sub>4</sub> emissions, or CH<sub>4</sub> hot spots ( $\geq$  7.4  $\mu$ g C m<sup>-2</sup> h<sup>-1</sup>) were observed during both measurement periods. CH<sub>4</sub> cold spots ( $\leq$  -20.1  $\mu$ g C m<sup>-2</sup> h<sup>-1</sup>) or higher CH<sub>4</sub> uptake occurred during the vegetation and frost-free period. Overall, the CV of CH<sub>4</sub> fluxes during the entire observation period was 4962%.

ER-CO<sub>2</sub> emissions during the measurement period ranged from 23.0 to 387.7 mg C m<sup>-2</sup> h<sup>-1</sup>, with a mean of 228.0  $\pm$  18.5 mg C m<sup>-2</sup> h<sup>-1</sup>, and a median of 226.0 mg C m<sup>-2</sup> h<sup>-1</sup> (Fig. 2e). Unlike N<sub>2</sub>O and CH<sub>4</sub> fluxes, CO<sub>2</sub> hot spots ( $\geq$  392.2 mg C m<sup>-2</sup> h<sup>-1</sup>) were only recorded during the vegetation and frost-free period. The CV of ER- CO<sub>2</sub> emissions was 49.3% during the entire observation period.









205

210

215

220

225

230

235



Figure 2: Seasonal variations in daily precipitation (source Danish Meteorological Institute, 2025) and volumetric moisture content at a soil depth of 0-5 cm (a), mean daily air temperature (source Danish Meteorological Institute, 2025) and soil temperature at a soil depth of 5 cm (b), as well as fluxes of soil nitrous oxide (N<sub>2</sub>O) (c), methane (CH<sub>4</sub>) (d) and ecosystem (i.e. soil and plant) respiration (CO<sub>2</sub> fluxes) (e) over the entire observation period from July to December, 2023. The vegetation and frost-free period spans from 20 July to 21 November, 2023, while the freeze-thaw period spans from 22 November to 31 December, 2023. In panels c-e, the black solid diamonds and lines inside the box represent the mean and median, respectively. The box borders represent the 75th and 25th percentiles, and the whisker caps represent the 95th and 5th percentiles. Grey circle points represent observation data, and the red and blue circle and hollow points represent hot spots and cold spots, respectively. The definition of hot and cold spots can be found in the Materials and Methods section. The dashed lines represent the zero line.

## 3.3 Spatial variability of N2O, CH4, and CO2 fluxes

The cumulative  $N_2O$  fluxes over the vegetation and frost-free period ranged from -0.01 to 9.96 kg N ha<sup>-1</sup> for all 56 sampling sites (Table S9). During the freeze-thaw period, the fluxes ranged from -0.01 to 0.74 kg N ha<sup>-1</sup>. On average, the soils at our sampling sites acted as a significant net source of atmospheric  $N_2O$ , with a mean of  $0.57 \pm 0.20$  kg N ha<sup>-1</sup>. The CV between the different sampling sites was 259%. The RF analysis showed that spatial variability in  $N_2O$  fluxes could be modeled with an overall performance of 87% using the variables SOC, silt content, distance to the nearest tree, soil temperature and grass height (Table S10 and Fig. S3). The model displayed no probability of cold spots in the study areas and 54% probability of hot spots (Table S10). Spatial variation in the predictions showed a higher probability of hotspots close to the artificial ponds and a lower probability in the northeast section of the park (Fig. 3a).

Cumulative CH<sub>4</sub> fluxes over the vegetation and frost-free period showed contrasted differences among the sampling sites (Table S9). That is, the cumulative CH<sub>4</sub> uptake was observed at 45 out of 56 sampling sites, ranging in magnitude from -0.83 to -0.04 kg C ha<sup>-1</sup>. The remaining 11 sampling sites were net sources of atmospheric CH<sub>4</sub>, ranging from 0.01 to 5.44 kg C ha<sup>-1</sup>. The CV between the different uptake sites was 60.5 % and the CV between the different source sites was 140.3%, both were lower than the CV of 3154 % between all the sampling sites. Based on the variables soil moisture, SOC, soil temperature, TN and distance to the nearest body of water, the RF model showed good predictive power for spatial variability of CH<sub>4</sub> fluxes, with the overall performance of 91% (Fig. S3 and Table S10). Moreover, the model was more accurate in predicting cold spots of CH<sub>4</sub> uptake (78%) than hot spots of CH<sub>4</sub> emissions (54%) (Table S10). The spatial predictions for our study areas showed a higher probability of hot spots closer to the artificial ponds and streams, particularly at two specific sites (Fig. 3b). However, the areas immediately adjacent to the water's edge were not necessarily identified as either hot spots or cold spots. Areas draining toward the artificial ponds showed the highest overall probability of becoming cold spots of CH<sub>4</sub> uptake over time, particularly in the northeastern and southern sections (Fig. 3c).

During the vegetation and frost-free periods, the cumulative ER-CO<sub>2</sub> emissions for the 56 sampling sites ranged from 0.7- 10.2 Mg C ha<sup>-1</sup>, with a mean of  $5.48 \pm 0.30$  Mg C ha<sup>-1</sup>. The CV between the different sampling sites was 40.3%. Using the variables soil temperature, distance to the nearest body of water, soil moisture and clay content, the RF model achieved a 67% performance for hot spot detection, but it did not show any cold spot probability (Table S10). Similar to the spatial variability of CH<sub>4</sub> emission hot spots, the RF model showed a higher probability of ER-CO<sub>2</sub> emission hot spots closer to the artificial ponds and streams (Fig. 3d).





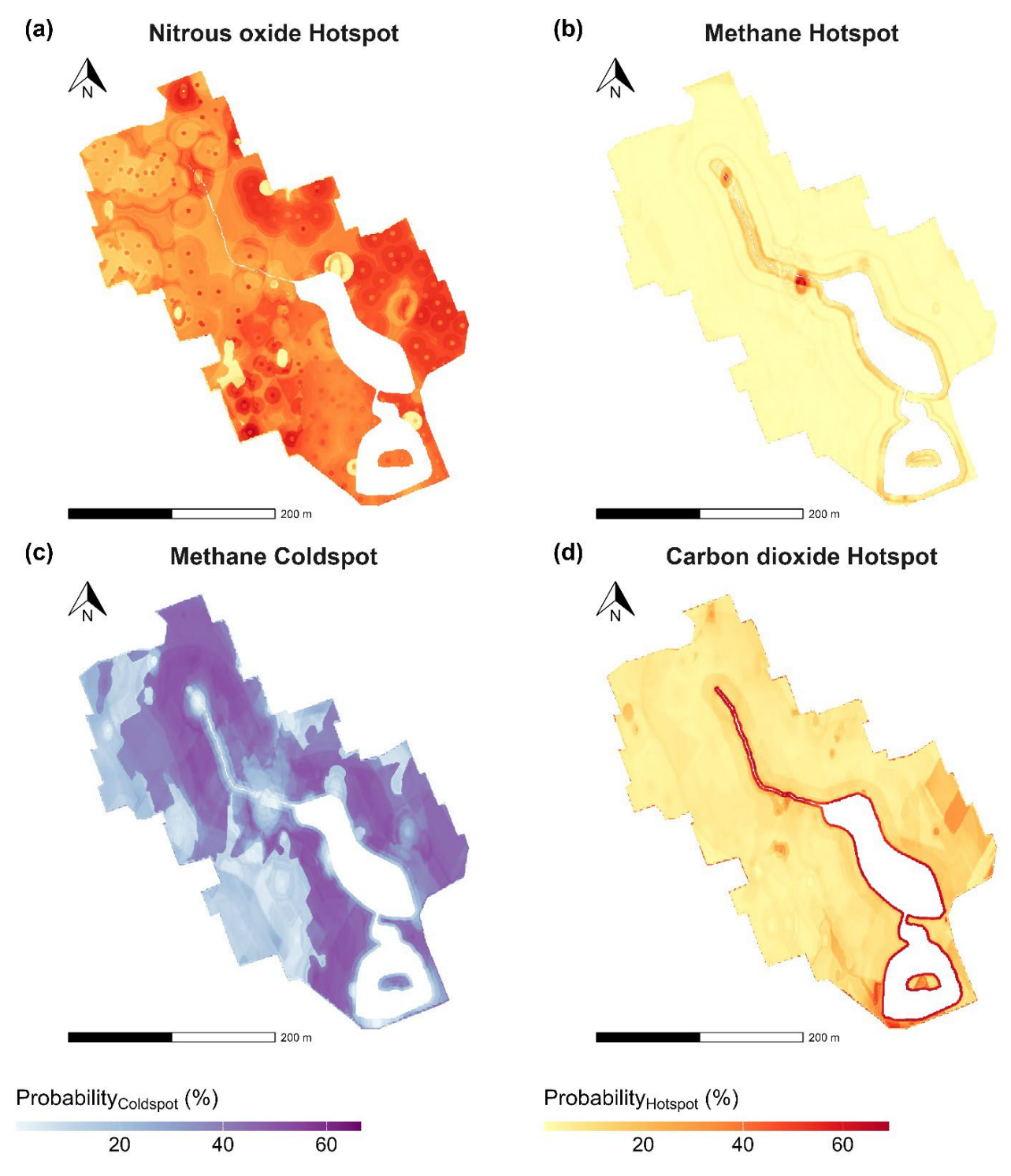


Figure 3: This map shows the area with the highest overall mean probability of being classified as nitrous oxide (N<sub>2</sub>O) emission hot spots(a), methane (CH<sub>4</sub>) emission hot spots(b), CH<sub>4</sub> uptake cold spots(c) and carbon dioxide (CO<sub>2</sub>) emission hot spots(d). The definition of hot and cold spots can be found in the Materials and Methods section.



245

250

255



# 3.4 Key factors driving the spatiotemporal variability

Although the simple regression analysis did not show a significant relationship between N<sub>2</sub>O fluxes and environmental and soil variables, the RF model, which considers the interactions between the variables could explain 80% of the variance in N<sub>2</sub>O fluxes (Fig. S3 and Table S10). Across the 56 sampling sites, the cumulative N<sub>2</sub>O fluxes were also negatively correlated with soil pH (Fig. 4a).

To clearly show the key factors controlling the CH<sub>4</sub> flux variations, we separated the data into CH<sub>4</sub> uptake rates and CH<sub>4</sub> emissions. Across the different uptake sites, the cumulative CH<sub>4</sub> uptake rates were negatively correlated with soil moisture, while positively correlated with the C/N ratio (Fig. 4c and 4d). During the measurement period, the daily CH<sub>4</sub> uptake rates also showed a negative relationship with soil moisture (Fig. 5a). Across the different source sites, the cumulative CH<sub>4</sub> emissions were positively correlated with soil moisture (Fig. 4e), SOC (Fig. 4g) and TN (Fig. 3h), while negatively correlated with soil BD (Fig. 4f). A multiple regression analysis of all the CH<sub>4</sub> data showed that cumulative CH<sub>4</sub> fluxes were significantly controlled by the combined effect of soil moisture (SM), soil temperature (ST) and SOC (i.e., cumulative CH<sub>4</sub> fluxes = -5.77 + 0.10SM + 0.17ST + 0.01SOC;  $R^2 = 0.54$ , p < 0.001).

Soil temperature showed significantly positive effects on both spatial and temporal variations of ER-CO<sub>2</sub> emissions (Fig. 4b and 5c). In addition, the daily ER-CO<sub>2</sub> emissions during the observation period were negatively correlated with soil moisture (Fig. 5b) and positively correlated with grass height (Fig. 5d).





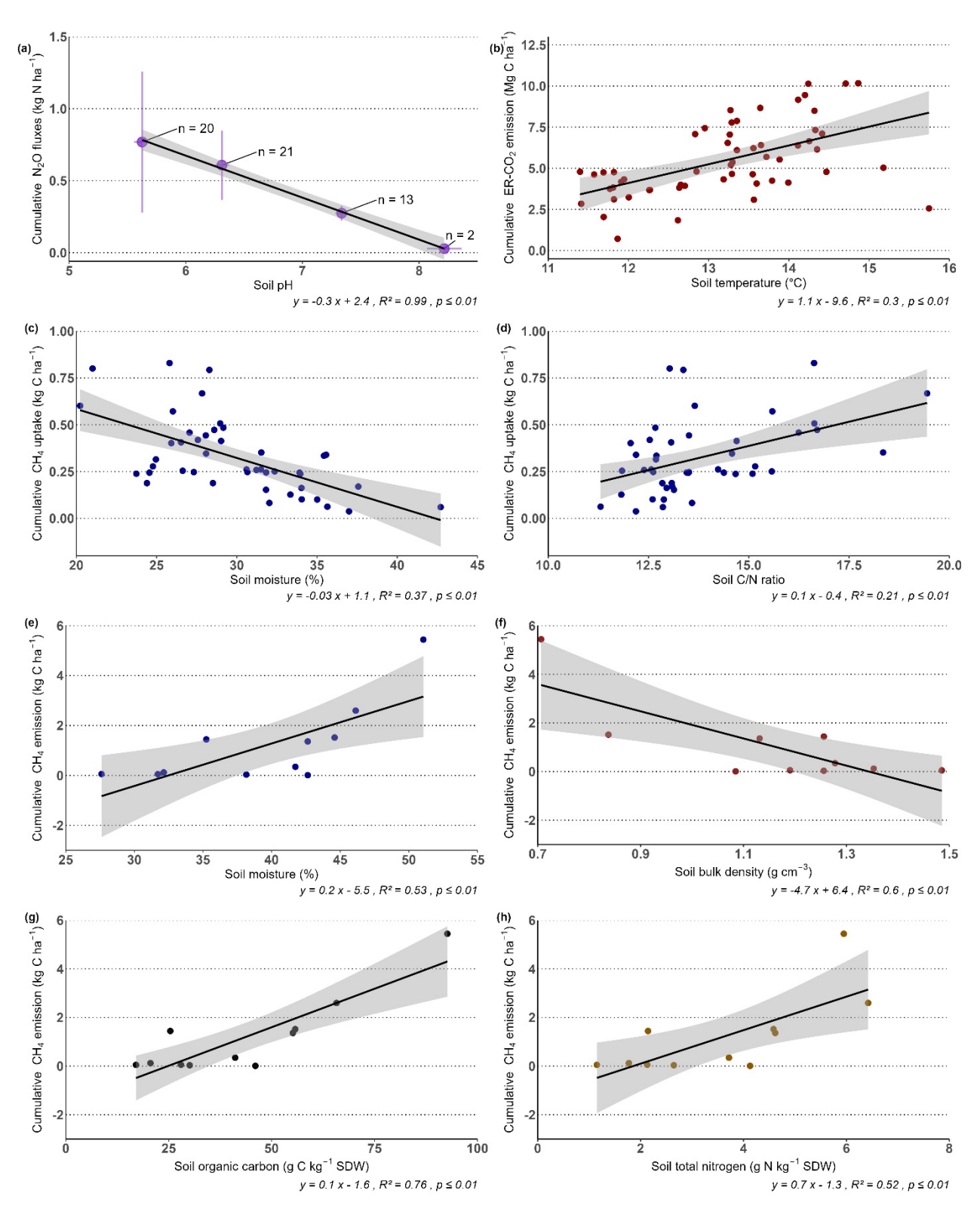






Figure 4: The relationships between cumulative nitrous oxide (N<sub>2</sub>O) fluxes and soil pH (a), between cumulative ecosystem respiration (ER-CO<sub>2</sub>) emissions and soil temperature (b), between cumulative methane (CH<sub>4</sub>) uptake and soil moisture (c) and soil C/N ratio (d), between cumulative CH<sub>4</sub> emissions and soil moisture (e), soil bulk density (f), soil organic carbon (g), and soil total nitrogen (h) across all the sampling sites.In panel a, soil pH was binned at a step width of 1 (i.e. 5.0-6.0, 6.0-7.0, 7.0-8.0 and >8.0), and points are given as mean values ± standard error, with numbers referring to the number of observations. SDW: soil dry weight. The shaded area of each panel represents the 95% confidence band.

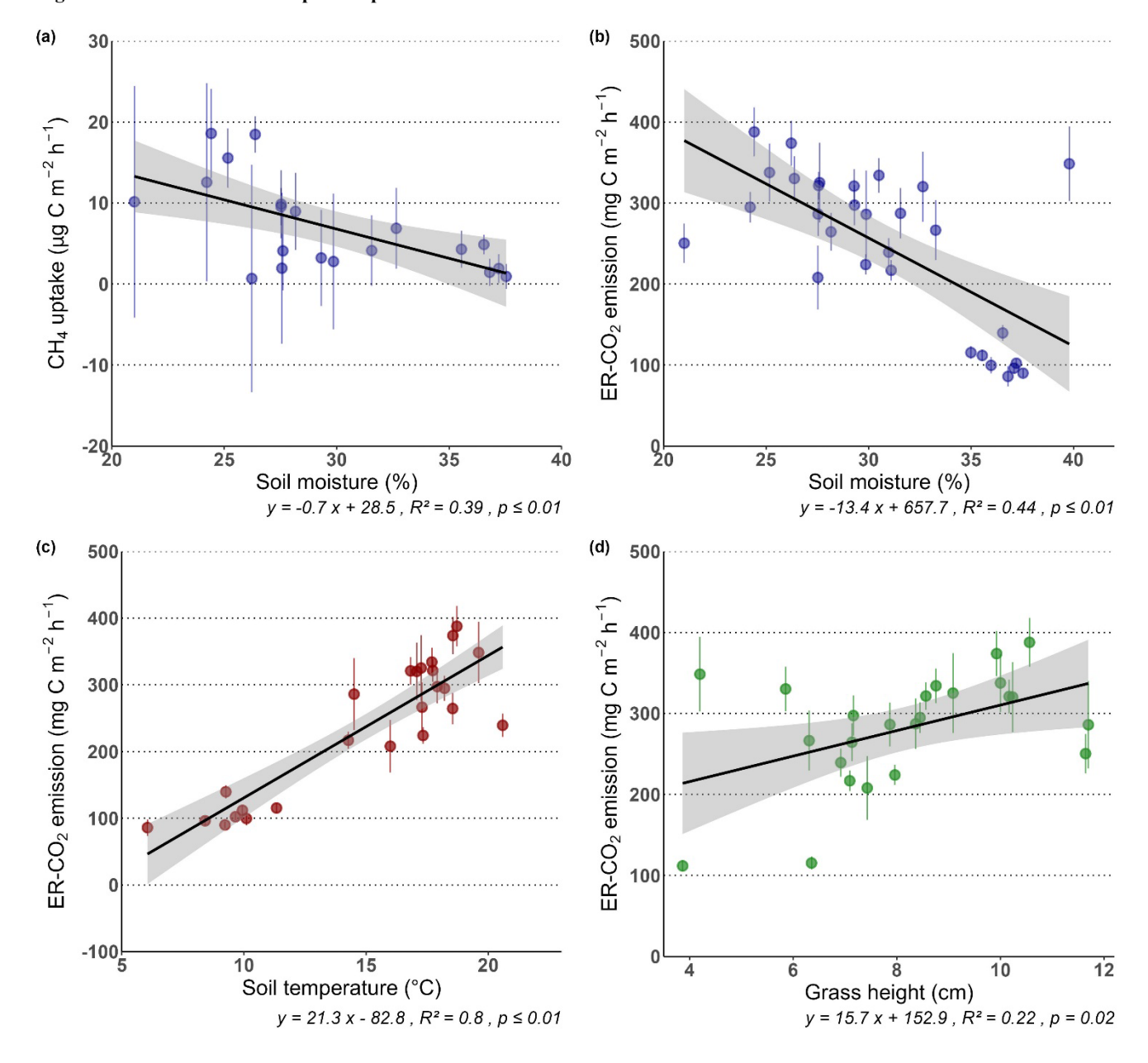


Figure 5: The relationships between methane (CH<sub>4</sub>) uptake and soil moisture (b), between ecosystem respiration (ER-CO<sub>2</sub>) emissions and soil moisture (b), soil temperature (c) and grass height (d) across the vegetation and frost-free periods. Points are





given as mean values  $\pm$  standard error across all the sampling sites at the same measurement time. The shaded area of each panel represents the 95% confidence band.

#### 4. Discussion

275

280

285

290

295

300

Urban green spaces play an important role in improving quality of life and developing a sustainable urban environment (Giannico et al., 2021; Semeraro et al., 2021; Jabbar et al., 2022). However, many urban green spaces in both developed and developing countries are under-represented in global C and N cycling studies. As global urbanization continues to expand, this contributes to high uncertainties in regional and national GHG budgets (Gao and O'Neill, 2020). In our study, we assessed soil GHG fluxes from an urban park in the Danish city of Aarhus during the vegetation growth and freeze-thaw periods. Our goal was to improve our understanding of the patterns and drivers of the temporal and spatial variability in these fluxes, as well as demonstrate the necessity of addressing spatial variability in studies of GHG fluxes from urban green areas.

## 4.1 Nitrous oxide (N2O) fluxes

Over the entire observation period, the mean of all measurements resulted in an average daily N<sub>2</sub>O emission of 23.8 µg N m<sup>-2</sup> h<sup>-1</sup> for the urban park. This value falls within the range (-1.1 to 84.5 μg N m<sup>-2</sup> h<sup>-1</sup>) reported for urban green spaces in China, Singapore, Australia, Europe and North America (Maggiotto et al., 2000; Livesley et al., 2010; Davis et al., 2015; LeMonte et al., 2016; Braun and Bremer, 2018; Riches et al., 2020; Stefane et al., 2021; Künnemann et al., 2023). However, our observed N<sub>2</sub>O emissions exhibit significant temporal and spatial variability, with CV values ranging from 45.6% and 259%. This high variability is consistent with that observed in other studies of forests, grasslands and agricultural systems (Kiese et al., 2003; Yao et al., 2009; van Delden et al., 2018; Wangari et al., 2022; Daelman et al., 2025). The highly dynamic nature of N2O fluxes is primarily because soil N2O fluxes are regulated by numerous abiotic and biotic factors that either fuel or restrain microbial processes (nitrification and denitrification) at various spatial and temporal scales (Butterbach-Bahl et al., 2013). For example, our regression analysis revealed a significant negative relationship between cumulative N<sub>2</sub>O emissions and soil pH (Fig. 4a). The optimal pH range for denitrifiers is often reported to be 6.5-8.0 (Knowles, 1981; Šimek and Cooper, 2002). Thus, any increase above the mean soil pH observed in our study (pH 6.37) should theoretically increase N<sub>2</sub>O production. However, at low soil pH levels, the reduction of N<sub>2</sub>O to N<sub>2</sub> by N<sub>2</sub>O reductase (nosZ) is substantially reduced, either due to the direct effect of pH on the assembly of N<sub>2</sub>O reductase or due to shifts in the soil denitrification community toward denitrifiers lacking the nosZ gene (Cûhel et al., 2010; Xu et al., 2020). In other words, the partitioning of N<sub>2</sub>O and N<sub>2</sub> during denitrification is affected by soil pH, with a higher proportion of N<sub>2</sub>O present in acidic conditions. On the contrary, microbial activity may increase at higher pH values, leading to higher N<sub>2</sub>O emissions. However, this may not be the case, as the N<sub>2</sub>O yield during denitrification decreases with increasing pH (Cûhel et al., 2010).

For the sites we investigated, the high spatiotemporal variability in soil N<sub>2</sub>O fluxes cannot be solely explained based on soil moisture status and/or temperature changes. Nevertheless, "hot moments" of soil N<sub>2</sub>O emissions were observed



305

310

315

320

325

330



during the freeze-thaw period. These data suggest that soil N<sub>2</sub>O fluxes are sensitive to changes in environmental factors, such as soil temperature changes, during the freeze-thaw period. Other studies have reported similar pulses of N<sub>2</sub>O fluxes during freeze-thaw periods in boreal and temperate ecosystems, including forests, grasslands and agricultural fields (Butterbach-Bahl et al., 2002; Luo et al., 2013; Wagner-Riddle et al., 2017). However, our observation of this phenomenon in urban green spaces is novel. Pulses of N<sub>2</sub>O emissions during freeze-thaw periods are generally attributed to the close coupling of microbial mineralization, nitrification, and denitrification, occurring under conditions in which the surface soil is close to moisture saturation, and increased availability of easily degradable C and N substrates. This can be due to the death of soil microbes from frost, as suggested by De Bruin et al., 2009.

Although our linear regression analysis did not reveal a significant relationship between soil temperature and  $N_2O$  fluxes, RF model identified soil temperature as one of the most influential predictors (Fig. S3). Despite the limited ability to accurately classify  $N_2O$  emission hot spots (Fig. 3a), the spatial probability maps indicate that large portions of the park show a moderate likelihood (39  $\pm$  13%) of becoming hot spots under specific conditions. This implies that hot spots are not confined to fixed locations but instead emerge dynamically in response to transient environmental triggers, such as freeze-thaw events or soil saturation. To improve hot spot prediction, we emphasize the need for higher-frequency flux measurements, particularly during periods of rapid environmental change and finer resolution of soil data (Helfenstein et al., 2024).

## 4.2 Methane (CH<sub>4</sub>) fluxes

During the observation period, the soils in the urban park were predominantly a weak sink for atmospheric CH<sub>4</sub> (-0.26 μg C m<sup>-2</sup> h<sup>-1</sup> on average over all measurements), though they sporadically changed from a sink to a source after rainfall events. This sink-to-source dynamic, driven by soil water status, is consistent with observations from an urban lawn in Australia (van Delden et al., 2018). Moreover, the magnitude of the mean CH<sub>4</sub> fluxes observed in our study was at the lower end of the reported uptake rates from urban green spaces in other European countries and the USA (Groffman and Pouyat, 2009; Bezyk et al., 2022; Trémeau et al., 2024). Regression analysis revealed a strong negative correlation between CH<sub>4</sub> uptake rates and soil moisture. However, no significant relationship was observed between CH<sub>4</sub> uptake rates and soil temperature. These results suggest that soil moisture is the dominant environmental driver of the temporal variability of CH<sub>4</sub> fluxes compared to temperature in this urban park. Similar results have been observed in many studies of urban green spaces or natural forests and grasslands (van Delden et al., 2018; Liu et al., 2019). Generally, soil moisture affects soil gas diffusion and the microbial populations that regulate the CH<sub>4</sub> dynamics (Potter et al., 1996; Smith et al., 2018; Bezyk et al., 2023). At high soil moisture contents, CH<sub>4</sub> uptake is usually limited by its diffusivity into the soil. These results suggest that future studies require high-temporal-resolution soil hydrological observations to better trace the dynamics of CH<sub>4</sub> fluxes.

In this study, cumulative CH<sub>4</sub> fluxes for all 56 sampling sites were used in the analyses of spatial variability (Table S9). The results showed that there was a striking difference in cumulative CH<sub>4</sub> fluxes among the sampling sites, i.e., CH<sub>4</sub> emissions occurred in 11 of the 56 sites. These significant CH<sub>4</sub> emissions are likely due to the predominance of soil water



335

340

345

350

355

360

365



saturation and accumulation of C substrates in topsoils, as sites functioning as net sources of CH<sub>4</sub> to the atmosphere were positioned closer to artificial ponds and streams within the urban park. Our regression analysis revealed that soil moisture was positively correlated with cumulative CH<sub>4</sub> emissions, while negatively correlated with cumulative CH<sub>4</sub> uptake (Fig. 4c and 4e). The opposite response of cumulative CH<sub>4</sub> fluxes to soil moisture status between source and sink sites is likely due to the fact that higher soil moisture contents suppress gas diffusion and increase the volume of anaerobic soil. This suppresses methanotrophy and stimulates methanogenesis, thereby reducing CH<sub>4</sub> oxidation and promoting CH<sub>4</sub> production (McLain and Ahmann, 2007; Praeg et al., 2014). Moreover, the cumulative CH<sub>4</sub> emissions increased with increasing SOC and TN. This corroborates previous findings that SOC and TN are important factors in controlling ecosystem CH<sub>4</sub> emissions because they can provide C and N substrates to methanogens and thus enhancing their activities and associated CH<sub>4</sub> production (Ma et al., 2020; Zhao and Zhuang, 2024). We noticed that the studied sites with higher SOC values typically have relatively low BD values. This could explain why cumulative CH<sub>4</sub> emissions decreased as BD increased in our study (Fig. 4f). Additionally, the cumulative CH<sub>4</sub> uptake was strongly and positively correlated with soil C/N ratios. Lower C/N ratios in urban soils likely support higher rates of N transformation, particularly mineralization and nitrification. However, increased soil N availability can inhibit methanotrophic activities and associate CH<sub>4</sub> oxidation (Steinkamp et al., 2000; Zhan et al., 2023). Considering all 56 sites together, the spatial variability of CH<sub>4</sub> fluxes was significantly regulated by the combined effects of soil moisture, temperature and SOC. Furthermore, these three variables were also included in the RF model to predict CH<sub>4</sub> hot and cold spots. Previous studies have similarly reported that soil moisture, temperature and C availability are the main drivers shaping the spatial patterns of CH<sub>4</sub> fluxes across heterogeneous landscapes (West et al., 1999; Olefeldt et al., 2013; Kaiser et al., 2018; Yu et al., 2019).

#### 4.3 Carbon dioxide (CO<sub>2</sub>) emissions

In this study, the average ER-CO<sub>2</sub> emissions were 228 mg C m<sup>-2</sup> h<sup>-1</sup> when using the arithmetic mean of all measurements. Our observed ER-CO<sub>2</sub> emissions are consistent with the reported range (142-298 mg C m<sup>-2</sup> h<sup>-1</sup>) for open lawns, treed lawns, and urban woodlands in France (Künnemann et al., 2023), but higher than the emissions recorded in urban woodlands (54-100 mg C m<sup>-2</sup> h<sup>-1</sup>) by Groffman et al (2009) and Chen et al. (2013). Over the entire observation period, ER-CO<sub>2</sub> emission variability was negatively correlated with soil moisture and positively correlated with soil temperature and grass height (Fig. 5b-d). Ecosystem respiration depends heavily on plant respiration and microbial decomposition. Grass height is a proxy for aboveground biomass and, consequently, has a positive effect on ER-CO<sub>2</sub> emissions. The positive correlation with aboveground biomass has been well documented in previous studies (Ding et al., 2007; Yao et al., 2013). High levels of soil moisture can restrict the availability of O<sub>2</sub> within the soil matrix, creating conditions conducive to anoxic processes, and resulting in reduced CO<sub>2</sub> emissions (Hao et al., 2025). Moreover, the SOC decomposition process is constrained by anoxia, which restricts the release of nutrients necessary for CO<sub>2</sub> formation (Keiluweit et al., 2017). Nevertheless, increases in soil temperature can alleviate limitations on plant function and the microbial decomposition of SOC. This promotes plant biomass accumulation, autotrophic and heterotrophic respiration and, thus, ecosystem respiration (i.e., ER-CO<sub>2</sub> emissions).



370

375

380

385

390

395



Across all the 56 sampling sites, our results showed that soil temperature was the dominant factor influencing the spatial variability in cumulative ER-CO<sub>2</sub> emissions, with a particularly strong effect in sites around artificial ponds. Furthermore, the RF model confirmed this pattern of CO<sub>2</sub> emissions across the landscape. That is, ER-CO<sub>2</sub> hotspots were concentrated around artificial ponds where grass heights were higher. As previously mentioned, elevated soil temperatures stimulate greater ER-CO<sub>2</sub> emissions by promoting vegetation growth under unlimited soil water conditions. These results suggest that future work should focus on integrating biomass estimates from remote sensing (Hoyos-Santillan et al., 2025). This could serve as an alternative to grass-height measurements, which are currently limited to sampling sites. In other words, integrating remote sensing of vegetation dynamics with gas flux monitoring could provide a scalable method of linking plant phenology with ER-CO<sub>2</sub> emission variability in urban green spaces.

In this study, we view the RF as a complement, rather than a replacement for empirical methods. For example, in this study, the RF helped identify the combined effects of multiple factors, such as soil temperature (CH<sub>4</sub>) and clay content (CO<sub>2</sub>), which were not always significant in empirical regressions. Combining these two approaches is especially valuable in the context of urban GHG budgets, where spatial heterogeneity and temporal variability complicate the process of upscaling and extrapolating from limited site measurements. This integration allows for more precise evaluations of the contribution of urban green spaces to city-scale GHG fluxes.

Practically speaking, city managers and policymakers could use these predictive frameworks to identify "hotspotprone" zones in urban parks. They could then direct targeted interventions to these zones rather than treating green spaces as homogeneous. This approach may increase the efficiency of climate mitigation actions by allocating management resources to areas where emissions are likely to be most intense. Beyond Aarhus, this framework could be adopted by other cities with similar green space structures, making it a relevant tool for integrating soil GHG fluxes into urban carbon accounting.

# 5. Conclusions

Despite the rapid urban sprawl occurring around the world, urban green spaces and their biogeochemical carbon and nitrogen cycles are still generally understudied. The limited urban soil GHG flux data available does not accurately reflect spatial and temporal variations in fluxes, resulting in GHG budgets with large uncertainties. This study provides insights into the spatiotemporal variability of soil CH<sub>4</sub> and N<sub>2</sub>O fluxes and ecosystem CO<sub>2</sub> emissions in an urban park located in a hilly landscape, based on measurements of vegetation growth and freeze-thaw periods across the 56 sites that vary in vegetation type and landscape position. On average, our results show that the soils in urban green spaces primarily function as a source of N<sub>2</sub>O and a weak sink of CH<sub>4</sub>. Moreover, our observations confirm significant temporal and spatial variations in soil CH<sub>4</sub> and N<sub>2</sub>O fluxes and ecosystem CO<sub>2</sub> emissions. This high variability is strongly related to changes in environmental and landscape parameters such as vegetation structure, soil hydrothermal conditions, pH and the availability of carbon and nitrogen. These findings underscore the necessity of additional measurement campaigns in urban green spaces. These campaigns should have an experimental design that allows for large spatial coverage and a high temporal sampling





frequency when determining soil fluxes. Based on our comprehensive observed datasets, however, we developed RF models to predict the probability of GHG hot spots and/or cold spots. While model performance varied depending on trace gas and driver complexity, the RF approach effectively captured the spatial heterogeneity and provided a scalable framework for mapping GHG fluxes across urban green spaces. Overall, our findings may allow for better scaling of GHG fluxes in urban green spaces and enable a more accurate assessment of how urbanization changes landscape fluxes.

- Author contribution. XB conducted the greenhouse gas, soil temperature, and soil moisture measurements, analyzed the data, and wrote the manuscript. TC measured soil pH, performed data analysis, conducted the machine learning part, and prepared Figure 1. JS assisted TC with the machine learning analysis, contributed to figure preparation (including Figure 3), and co-wrote the manuscript. KBB reviewed and edited the manuscript. ZSY contributed to data analysis, writing, and manuscript revision.
- 410 **Acknowledgments.** We thank our technicians Lars Norge Andreassen and Joakim Voltelen Klausen for their help with the measurements and running the equipment.

**Financial support.** This research has been supported by "Pioneer Center for Research in Sustainable Agricultural Futures" (Land-CRAFT), DNRF grant number P2, Aarhus University, Denmark.

#### References

- Alletto, L. and Coquet, Y.: Temporal and spatial variability of soil bulk density and near-saturated hydraulic conductivity under two contrasted tillage management systems, Geoderma, 152, 85–94, https://doi.org/10.1016/j.geoderma.2009.05.023, 2009.
  - Best, E. K.: An automated method for determining nitrate-nitrogen in soil extracts, Qld. J. Agric. Anim. Sci., 33, 161–166, 1976
- 420 Bezyk, Y., Dorodnikov, M., Górka, M., Sówka, I., and Sawiński, T.: Temperature and soil moisture control CO<sub>2</sub> flux and CH<sub>4</sub> oxidation in urban ecosystems, Geochem., 83, 125989, https://doi.org/10.1016/j.chemer.2023.125989, 2023.
  - Bezyk, Y., Sówka, I., Górka, M., and Nęcki, J.: Spatial and temporal patterns of methane uptake in the urban environment, Urban Clim., 41, 101073, https://doi.org/10.1016/j.uclim.2021.101073, 2022.
- Braun, R. C. and Bremer, D. T.: Nitrous oxide emissions from turfgrass receiving different irrigation amounts and nitrogen fertilizer forms, Crop Sci., 58, 1762–1775, https://doi.org/10.2135/cropsci2017.11.0688, 2018.
  - Butterbach-Bahl, K., Baggs, E. M., Dannenmann, M., Kiese, R., and Zechmeister-Boltenstern, S.: Nitrous oxide emissions from soils: how well do we understand the processes and their controls?, Philos. Trans. R. Soc. Lond. B Biol. Sci., 368, 20130122, https://doi.org/10.1098/rstb.2013.0122, 2013.
- Butterbach-Bahl, K., Rothe, A., and Papen, H.: Effect of tree distance on N<sub>2</sub>O and CH<sub>4</sub> fluxes from soils in temperate forest ecosystems, Plant Soil, 240, 91–103, https://doi.org/10.1023/A:1015828701885, 2002.





- Cardinali, M., Beenackers, M. A., Fleury-Bahi, G., Bodénan, P., Petrova, M. T., van Timmeren, A., and Pottgiesser, U.: Examining green space characteristics for social cohesion and mental health outcomes: A sensitivity analysis in four European cities, Urban For. Urban Green., 93, 128230, https://doi.org/10.1016/j.ufug.2024.128230, 2024.
- Chen, W., Jia, X., Zha, T., Wu, B., Zhang, Y., Li, C., Wang, X., He, G., Yu, H., and Chen, G.: Soil respiration in a mixed urban forest in China in relation to soil temperature and water content, Eur. J. Soil Biol., 54, 63–68, https://doi.org/10.1016/j.ejsobi.2012.10.001, 2013.
  - Crooke, W. M. and Simpson, W. E.: Determination of ammonium in Kjeldahl digests of crops by an automated procedure, J. Sci. Food Agric., 22, 9–10, 1971.
- Conrad, R.: Soil microorganisms as controllers of atmospheric trace gases (H<sub>2</sub>, CO, CH<sub>4</sub>, OCS, N<sub>2</sub>O, and NO), Microbiol. 440 Rev., 60, 609–640, https://doi.org/10.1128/mr.60.4.609-640.1996, 1996.
  - Daelman, R., Bauters, M., Barthel, M., Bulonza, E., Lefevre, L., Mbifo, J., Six, J., Butterbach-Bahl, K., Wolf, B., Kiese, R., and Boeckx, P.: Spatiotemporal variability of CO<sub>2</sub>, N<sub>2</sub>O and CH<sub>4</sub> fluxes from a semi-deciduous tropical forest soil in the Congo Basin, Biogeosciences, 22, 1529–1542, https://doi.org/10.5194/bg-22-1529-2025, 2025.
- Danish Meteorological Institute: https://www.dmi.dk/lokationarkiv/show/DK/2624652/Aarhus/#arkiv, last access: 05 March 2025.
  - Davis, M. P., David, M. B., Voigt, T. B., and Mitchell, C. A.: Effect of nitrogen addition on Miscanthus × giganteus yield, nitrogen losses, and soil organic matter across five sites, Glob. Change Biol. Bioenergy, 7, 1222–1231, https://doi.org/10.1111/gcbb.12217, 2015.
- Ding, W., Meng, L., Yin, Y., Cai, Z., and Zheng, X.: CO<sub>2</sub> emission in an intensively cultivated loam as affected by long-term application of organic manure and nitrogen fertilizer, Soil Biol. Biochem., 39, 669–679, https://doi.org/10.1016/j.soilbio.2006.09.024, 2007.
  - Edmondson, J., Stott, I., Davies, Z., Gaston, K. J., and Leake, J. R.: Soil surface temperatures reveal moderation of the urban heat island effect by trees and shrubs, Sci. Rep., 6, 33708, https://doi.org/10.1038/srep33708, 2016.
- Feng, Z., Wang, L., Wan, X., Yang, J., Peng, Q., Liang, T., Wang, Y., Zhong, B., and Rinklebe, J.: Responses of soil greenhouse gas emissions to land use conversion and reversion a global meta-analysis, Glob. Change Biol., 28, 6665–6678, https://doi.org/10.1111/gcb.16370, 2022.
  - Gao, J. and O'Neill, B. C.: Mapping global urban land for the 21st century with data-driven simulations and Shared Socioeconomic Pathways, Nat. Commun., 11, 2302, https://doi.org/10.1038/s41467-020-15788-7, 2020.
- Gao, H., Tian, H., Zhang, Z., and Xia, X.: Warming-induced greenhouse gas fluxes from global croplands modified by agricultural practices: A meta-analysis, Sci. Total Environ., 820, 153288, https://doi.org/10.1016/j.scitotenv.2022.153288, 2022.
  - Giannico, V., Spano, G., Elia, M., D'Este, M., Sanesi, G., and Lafortezza, R.: Green spaces, quality of life, and citizen perception in European cities, Environ. Res., 196, 110922, https://doi.org/10.1016/j.envres.2021.110922, 2021.



495



- Groffman, P. M. and Pouyat, R. V.: Methane uptake in urban forests and lawns, Environ. Sci. Technol., 43, 5229–5235, https://doi.org/10.1021/es803720h, 2009.
  - Groffman, P. M., Williams, C. O., Pouyat, R. V., Band, L. E., and Yesilonis, I. D.: Nitrate leaching and nitrous oxide flux in urban forests and grasslands, J. Environ. Qual., 38, 1848–1860, https://doi.org/10.2134/jeq2008.0521, 2009.
  - Hao, Y., Mao, J., Bachmann, C. M., Hoffman, F. M., Koren, G., Chen, H., Tian, H., Liu, J., Tao, J., Tang, J., Li, L., Liu, L., Apple, M., Shi, M., Jin, M., Zhu, Q., Kannenberg, S., Shi, X., Zhang, X., Wang, Y., Fang, Y., and Dai, Y.: Soil moisture
- 470 controls over carbon sequestration and greenhouse gas emissions: a review, NPJ Clim. Atmos. Sci., 8, 16, https://doi.org/10.1038/s41612-024-00888-8, 2025.
  - Helfenstein, A., Mulder, V. L., Hack-ten Broeke, M. J. D., van Doorn, M., Teuling, K., Walvoort, D. J. J., and Heuvelink, G. B. M.: BIS-4D: mapping soil properties and their uncertainties at 25 m resolution in the Netherlands, Earth Syst. Sci. Data, 16, 2941–2970, https://doi.org/10.5194/essd-16-2941-2024, 2024.
- Hensen, A., Skiba, U., and Famulari, D.: Low cost and state of the art methods to measure nitrous oxide emissions, Environ. Res. Lett., 8, 025022, https://doi.org/10.1088/1748-9326/8/2/025022, 2013.
  - Hoyos-Santillan, J., Miranda, A., Chavarría, J., Hormazabal, C., Mola-Yudego, B., and González-Mahecha, E.: Plot- and landscape-level estimates of tree biomass and carbon stocks in Panama's mangrove Important Bird Areas, Sci. Data, 12, 1016, https://doi.org/10.1038/s41597-025-05354-5, 2025.
- 480 IPCC: Anthropogenic and natural radiative forcing, in: Climate Change 2013: The Physical Science Basis. Contribution of Working Group I to the Fifth Assessment Report of the Intergovernmental Panel on Climate Change, edited by: Stocker, T. F., Qin, D., Plattner, G. K., Tignor, M., Allen, S. K., Boschung, J., and Midgley, P. M., Cambridge University Press, Cambridge, United Kingdom and New York, NY, USA, 659–740, https://doi.org/10.1017/CBO9781107415324.004, 2013.
  IPCC: Global carbon and other biogeochemical cycles and feedbacks, in: Climate Change 2021: The Physical Science Basis.
- Contribution of Working Group I to the Sixth Assessment Report of the Intergovernmental Panel on Climate Change, edited by: Canadell, J. G., Monteiro, P. M. S., Costa, M. H., Cotrim da Cunha, L., Cox, P. M., Eliseev, A. V., Henson, S., Ishii, M., Jaccard, S., Koven, C., Lohila, A., Patra, P. K., Piao, S., Rogelj, J., Syampungani, S., Zaehle, S., and Zickfeld, K., Cambridge University Press, Cambridge, United Kingdom and New York, NY, USA, 673–816, https://doi.org/10.1017/9781009157896.007, 2021.
- Jabbar, M., Yusoff, M. M., and Shafie, A.: Assessing the role of urban green spaces for human well-being: a systematic review, GeoJournal, 87, 4405–4423, https://doi.org/10.1007/s10708-021-10474-7, 2022.
  - Jeong, M., Bae, J., and Yoo, G.: Urban roadside greenery as a carbon sink: systematic assessment considering understory shrubs and soil respiration, Sci. Total Environ., 927, 172286, https://doi.org/10.1016/j.scitotenv.2024.172286, 2024.
  - Kaiser, K. E., McGlynn, B. L., and Dore, J. E.: Landscape analysis of soil methane flux across complex terrain,
- Karvinen, E., Backman, L., Järvi, L., and Kulmala, L.: Soil respiration across a variety of tree-covered urban green spaces in Helsinki, Finland, SOIL, 10, 381–406, https://doi.org/10.5194/soil-10-381-2024, 2024.

Biogeosciences, 15, 3143–3167, https://doi.org/10.5194/bg-15-3143-2018, 2018.



515



- Kaye, J. P., Groffman, P. M., Grimm, N. B., Baker, L. A., and Pouyat, R. V.: A distinct urban biogeochemistry?, Trends Ecol. Evol., 21, 192–199, https://doi.org/10.1016/j.tree.2005.12.006, 2006.
- 500 Kaye, J. P., Burke, I. C., Mosier, A. R., and Guerschman, J. P.: Methane and nitrous oxide fluxes from urban soils to the atmosphere, Ecol. Appl., 14, 975–981, 2004.
  - Keiluweit, M., Wanzek, T., Kleber, M., Nico, P. S., and Fendorf, S.: Anaerobic microsites have an unaccounted role in soil carbon stabilization, Nat. Commun., 8, 1771, https://doi.org/10.1038/s41467-017-01406-6, 2017.
- Kiese, R., Hewett, B., Graham, A., and Butterbach-Bahl, K.: Seasonal variability of N<sub>2</sub>O emissions and CH<sub>4</sub> uptake by tropical rainforest soils of Queensland, Australia, Glob. Biogeochem. Cycles, 17, 1043, https://doi.org/10.1029/2002GB002014, 2003.
  - Knowles, R.: Denitrification, Microbiol. Rev., 46, 43-70, https://doi.org/10.1128/mr.46.1.43-70.1982, 1982.
  - Künnemann, T., Cannavo, P., Guérin, V., and Guénon, R.: Soil CO<sub>2</sub>, CH<sub>4</sub> and N<sub>2</sub>O fluxes in open lawns, treed lawns and urban woodlands in Angers, France, Urban Ecosyst., 26, 1659–1672, https://doi.org/10.1007/s11252-023-01407-y, 2023.
- LeMonte, J. J., Jolley, V. D., Summerhays, J. S., Terry, R. E., and Hopkins, B. G.: Polymer coated urea in turfgrass maintains vigor and mitigates nitrogen's environmental impacts, PLoS ONE, 11, e0146761, https://doi.org/10.1371/journal.pone.0146761, 2016.
  - Liu, H., Miao, Y., Chen, Y., Shen, Y., You, Y., Wang, Z., and Gang, C.: Responses of soil greenhouse gas fluxes to land management in forests and grasslands: a global meta-analysis, Sci. Total Environ., 967, 178773,
  - Liu, L., Estiarte, M., and Peñuelas, J.: Soil moisture as the key factor of atmospheric CH<sub>4</sub> uptake in forest soils under environmental change, Geoderma, 355, 113920, https://doi.org/10.1016/j.geoderma.2019.113920, 2019.
    - Livesley, S. J., Dougherty, B. J., Smith, A. J., Navaud, D., Wylie, L. J., and Arndt, S. K.: Soil-atmosphere exchange of carbon dioxide, methane and nitrous oxide in urban garden systems: impact of irrigation, fertiliser and mulch, Urban
- 520 Ecosyst., 13, 273–293, https://doi.org/10.1007/s11252-009-0119-6, 2010.

https://doi.org/10.1016/j.scitotenv.2025.178773, 2025.

- Luo, G. J., Kiese, R., Wolf, B., and Butterbach-Bahl, K.: Effects of soil temperature and moisture on methane uptake and nitrous oxide emissions across three different ecosystem types, Biogeosciences, 10, 3205–3219, https://doi.org/10.5194/bg-10-3205-2013, 2013.
- Ma, W., Li, G., Wu, J., Xu, G., and Wu, J.: Respiration and CH<sub>4</sub> fluxes in Tibetan peatlands are influenced by vegetation degradation, Catena, 195, 104789, https://doi.org/10.1016/j.catena.2020.104789, 2020.
  - Maggiotto, S. R., Webb, J. A., Wagner-Riddle, C., and Thurtell, G. W.: Nitrous and nitrogen oxide emissions from turfgrass receiving different forms of nitrogen fertilizer, J. Environ. Qual., 29, 621–630, https://doi.org/10.2134/jeq2000.00472425002900020033x, 2000.
- McLain, J. E. T. and Ahmann, D. M.: Increased moisture and methanogenesis contribute to reduced methane oxidation in elevated CO<sub>2</sub> soils, Biol. Fertil. Soils, 44, 623–631, https://doi.org/10.1007/s00374-007-0246-2, 2008.





- Nyang'au, J. O., Sørensen, P., and Møller, H. B.: Nitrogen availability in digestates from full-scale biogas plants following soil application as affected by operation parameters and input feedstocks, Bioresour. Technol. Rep., 24, 101675, https://doi.org/10.1016/j.biteb.2023.101675, 2023.
- Olefeldt, D., Turetsky, M. R., Crill, P. M., and McGuire, A. D.: Environmental and physical controls on northern terrestrial methane emissions across permafrost zones, Glob. Change Biol., 19, 589–603, https://doi.org/10.1111/gcb.12071, 2013.
  - Pan, B., Qian, Z., Xu, Z., Yang, J., Tao, B., Sun, X., Xu, X., Yu, Y., Wang, J., and Tao, X.: Edaphic factors mediate the responses of forest soil respiration and its components to nitrogen deposition along an urban–rural gradient, Sci. Total Environ., 946, 174423, https://doi.org/10.1016/j.scitotenv.2024.174423, 2024.
- Pedersen, A. S., Petersen, K. S., and Jensen, T. F.: Jordartskort over Danmark (Midtjylland) [Soil Map of Denmark (Centre Part)], Danmarks Geol. Unders., Miljøministeriet, 1989.
  - Potter, C. S., Davidson, E. A., and Verchot, L. V.: Estimation of global biogeochemical controls and seasonality in soil methane consumption, Chemosphere, 32, 2219–2246, https://doi.org/10.1016/0045-6535(96)00119-1, 1996.
  - Poulsen, A. H., Sørensen, M., Hvidtfeldt, U. A., Ketzel, M., Christensen, J. H., Brandt, J., Frohn, L. M., Massling, A., Khan, J., Münzel, T., and Raaschou-Nielsen, O.: Concomitant exposure to air pollution, green space and noise, and risk of
- 545 myocardial infarction: a cohort study from Denmark, Eur. J. Prev. Cardiol., 31, 131–141, https://doi.org/10.1093/eurjpc/zwad306, 2024.
  - Praeg, N., Wagner, A. O., and Illmer, P.: Effects of fertilisation, temperature and water content on microbial properties and methane production and methane oxidation in subalpine soils, Eur. J. Soil Biol., 65, 96–106, https://doi.org/10.1016/j.ejsobi.2014.10.002, 2014.
- Ravishankara, A. R., Daniel, J. S., and Portmann, R. W.: Nitrous oxide (N<sub>2</sub>O): the dominant ozone-depleting substance emitted in the 21st century, Science, 326, 123–125, https://doi.org/10.1126/science.1176985, 2009.
  - Riches, D., Porter, I., Dingle, G., Gendall, A., and Grover, S.: Soil greenhouse gas emissions from Australian sports fields, Sci. Total Environ., 707, 134420, https://doi.org/10.1016/j.scitotenv.2019.134420, 2020.
- Steinkamp, R., Butterbach-Bahl, K., and Papen, H.: Methane oxidation by soils of an N limited and N fertilized spruce forest in the Black Forest, Germany, Soil Biol. Biochem., 33, 145–153, https://doi.org/10.1016/S0038-0717(00)00124-3, 2001.
  - Schjønning, P., Lamandé, M., De Pue, J., Cornelis, W. M., Labouriau, R., and Keller, T.: The challenge in estimating soil compressive strength for use in risk assessment of soil compaction in field traffic, in: *Advances in Agronomy*, edited by: Sparks, D. L., Academic Press, 178, 61–105, https://doi.org/10.1016/bs.agron.2022.11.003, 2023.
- Schofield, R. K. and Taylor, A. W.: The measurement of soil pH, Soil Sci. Soc. Am. J., 19, 164–167, 560 https://doi.org/10.2136/sssaj1955.03615995001900020013x, 1955.
  - Semeraro, T., Scarano, A., Buccolieri, R., Santino, A., and Aarrevaara, E.: Planning of urban green spaces: an ecological perspective on human benefits, Land, 10, 105, https://doi.org/10.3390/land10020105, 2021.
  - Šimek, M. and Cooper, J. E.: The influence of soil pH on denitrification: progress towards the understanding of this interaction over the last 50 years, Eur. J. Soil Sci., 53, 345–354, https://doi.org/10.1046/j.1365-2389.2002.00461.x, 2002.



595



- Smith, K. A., Ball, T., Conen, F., Dobbie, K. E., Massheder, J., and Rey, A.: Exchange of greenhouse gases between soil and atmosphere: interactions of soil physical factors and biological processes, Eur. J. Soil Sci., 69, 10–20, https://doi.org/10.1111/ejss.12539, 2018.
  - Statistics Denmark: Table BEF44: population of Odense per January 1, 2012, https://www.statistikbanken.dk/BEF44, last access: 10 May 2025.
- 570 Stefaner, K., Ghosh, S., Mohd Yusof, M. L., Ibrahim, H., Leitgeb, E., Schindlbacher, A., and Kitzler, B.: Soil greenhouse gas fluxes from a humid tropical forest and differently managed urban parkland in Singapore, Sci. Total Environ., 786, 147305, https://doi.org/10.1016/j.scitotenv.2021.147305, 2021.
  - Trémeau, J., Olascoaga, B., Backman, L., Karvinen, E., Vekuri, H., and Kulmala, L.: Lawns and meadows in urban green space a comparison from perspectives of greenhouse gases, drought resilience and plant functional types, Biogeosciences,
- 575 21, 949–972, https://doi.org/10.5194/bg-21-949-2024, 2024.
  - van Delden, L., Rowlings, D. W., Scheer, C., and Grace, P. R.: Urbanisation-related land use change from forest and pasture into turf grass modifies soil nitrogen cycling and increases N<sub>2</sub>O emissions, Biogeosciences, 13, 6095–6106, https://doi.org/10.5194/bg-13-6095-2016, 2016.
- van Delden, L., Rowlings, D. W., Scheer, C., De Rosa, D., and Grace, P. R.: Effect of urbanization on soil methane and nitrous oxide fluxes in subtropical Australia, Glob. Change Biol., 24, 5695–5707, https://doi.org/10.1111/gcb.14444, 2018.
  - Vasenev, V. and Kuzyakov, Y.: Urban soils as hot spots of anthropogenic carbon accumulation: review of stocks, mechanisms and driving factors, Land Degrad. Dev., 29, 1607–1622, https://doi.org/10.1002/ldr.2944, 2018.
  - Wagner-Riddle, C., Congreves, K. A., Abalos, D., Berg, A. A., Brown, S. E., Ambadan, J. T., Gao, X., and Tenuta, M.: Globally important nitrous oxide emissions from croplands induced by freeze–thaw cycles, Nat. Geosci., 10, 279–283, https://doi.org/10.1038/ngeo2907, 2017.
  - Walkiewicz, A., Bulak, P., Khalil, M. I., and others: Assessment of soil CO<sub>2</sub>, CH<sub>4</sub>, and N<sub>2</sub>O fluxes and their drivers, and their contribution to the climate change mitigation potential of forest soils in the Lublin region of Poland, Eur. J. For. Res., 144, 29–52, https://doi.org/10.1007/s10342-024-01739-0, 2025.
- Wangari, E. G., Mwanake, R. M., Kraus, D., Werner, C., Gettel, G. M., Kiese, R., and others: Number of chamber measurement locations for accurate quantification of landscape-scale greenhouse gas fluxes: importance of land use, seasonality, and greenhouse gas type, J. Geophys. Res.-Biogeosci., 127, e2022JG006901, https://doi.org/10.1029/2022JG006901, 2022.
  - Wangari, E. G., Mwanake, R. M., Houska, T., Kraus, D., Gettel, G. M., Kiese, R., Breuer, L., and Butterbach-Bahl, K.: Identifying landscape hot and cold spots of soil greenhouse gas fluxes by combining field measurements and remote sensing data, Biogeosciences, 20, 5029–5067, https://doi.org/10.5194/bg-20-5029-2023, 2023.
  - West, A. E., Brooks, P. D., Fisk, M. C., Smith, L. K., Holland, E. A., Jaeger, C. H. III, Babcock, S., Lai, R. S., and Schmidt, S. K.: Landscape patterns of CH<sub>4</sub> fluxes in an alpine tundra ecosystem, Biogeochemistry, 45, 243–264, https://doi.org/10.1007/BF00993002, 1999.





- Xu, X., Liu, Y., Singh, B. P., Yang, Q., Zhang, Q., Wang, H., Xia, Z., Di, H., Singh, B. K., Xu, J., and Li, Y.: NosZ clade II rather than clade I determine in situ N<sub>2</sub>O emissions with different fertilizer types under simulated climate change and its legacy, Soil Biol. Biochem., 150, 107974, https://doi.org/10.1016/j.soilbio.2020.107974, 2020.
  - Yao, Z., Zheng, X., Wang, R., and others: Greenhouse gas fluxes and NO release from a Chinese subtropical rice—winter wheat rotation system under nitrogen fertilizer management, J. Geophys. Res.-Biogeosci., 118, 623–638, https://doi.org/10.1002/jgrg.20061, 2013.
- Yao, Z., Zheng, X., Xie, B., Liu, C., Mei, B., Dong, H., Butterbach-Bahl, K., and Zhu, J.: Comparison of manual and automated chambers for field measurements of N<sub>2</sub>O, CH<sub>4</sub>, and CO<sub>2</sub> fluxes from cultivated land, Atmos. Environ., 43, 1888–1896, https://doi.org/10.1016/j.atmosenv.2008.12.031, 2009.
  - Yu, L., Zhu, J., Zhang, X., Wang, Z., Dörsch, P., and Mulder, J.: Humid subtropical forests constitute a net methane source: a catchment-scale study, J. Geophys. Res.-Biogeosci., 124, 2927–2942, https://doi.org/10.1029/2019JG005210, 2019.
- Zhan, Y., Yao, Z., Groffman, P. M., Xie, J., Wang, Y., Li, G., Zheng, X., and Butterbach-Bahl, K.: Urbanization can accelerate climate change by increasing soil N<sub>2</sub>O emission while reducing CH<sub>4</sub> uptake, Glob. Change Biol., 29, 3489–3502, https://doi.org/10.1111/geb.16652, 2023.
  - Zhang, M., Weng, S., Gao, H., Liu, L., Li, J., and Zhou, X.: Urbanization degree rather than methanotrophic abundance decreases soil CH<sub>4</sub> uptake, Geoderma, 404, 115368, https://doi.org/10.1016/j.geoderma.2021.115368, 2021.
- Zhao, B. and Zhuang, Q.: Nitrogen cycling feedback on carbon dynamics leads to greater CH<sub>4</sub> emissions and weaker cooling effect of northern peatlands, Glob. Biogeochem. Cycles, 38, e2023GB007978, https://doi.org/10.1029/2023GB007978, 2024.